Journal of Cleaner Production 372 (2022) 133671

Contents lists available at ScienceDirect

Journal of Cleaner Production

journal homepage: www.elsevier.com/locate/jclepro

Cement encapsulation processes to mitigate the risks posed by different types of antimony-bearing mine waste

E. Álvarez-Ayuso [a,*], A. Murciego [b], M.A. Rodríguez [c], R. Mosser-Ruck [d]

[a] Department of Environmental Geochemistry, IRNASA (CSIC), C/ Cordel de Merinas 40-52, 37008, Salamanca, Spain
[b] Department of Geology, Salamanca University, Plza. de los Caídos s/n, 37008, Salamanca, Spain
[c] Department of Environmental Resources Analysis, Extremadura University, Avda. Elvas s/n, 06071, Badajoz, Spain
[d] Georessources UMR 7359 CNRS-UL, Université de Lorraine, BP 70239, Vandœuvre-lès-Nancy, 54506, Cedex, France

ARTICLE INFO

Handling editor. M.T. Moreira

Keywords:
Sb
Cementation
Leaching
Mine waste rocks
Mine tailings
Smelting waste

ABSTRACT

In this study cement encapsulation processes of different types of mine waste generated from the exploitation of Sb ore deposits were evaluated as a way to manage them and avoid further environmental pollution and the negative impact on surrounding ecosystems. For this purpose, Sb-bearing mine waste rocks, mine tailings, and smelting waste were subjected to cementation processes using Portland cement/calcium hydroxide as binder and different binder:mine waste ratios (10:90–80:20 wt%). The encapsulated materials were characterized for their mechanical behavior (compressive strength test), leaching properties (batch shaking and tank leaching tests), and mineralogical and chemical composition by X-ray powder diffraction, scanning electron microscopy, and electron microprobe analysis. A binder:mine waste ratio of 40:60 wt% was found appropriate to decrease the leachable Sb concentrations at levels below the limit for acceptance at non-hazardous waste landfills. Diffusion was the main mechanism controlling Sb leaching. The obtained effective diffusion coefficients and developed compressive strengths indicate that the encapsulated materials were suitable for disposal. Therefore, according to their leaching and strength characteristics, the encapsulated mine wastes derived using the indicated conditions could be deposited at landfills for non-hazardous waste, thus minimizing the environmental hazards caused by their accumulation in the mine surrounding areas. Additionally, according to the Dutch legislation on the use of waste materials in the built sector, some formulations of encapsulated mine tailings already met the Sb leaching requirement for open (un-insulated) construction applications. Therefore, Sb-bearing mine wastes, especially mine tailings, also present a great potential to be recycled as substitutes for natural aggregates in concrete in construction applications. Antimony was mostly preserved in the original Sb-bearing phases [Fe and Sb (oxy-hydr)oxides and tripuhyite] after the encapsulation processes. Of compounds resulting from the hydration of Portland cement, C-(A)-S-H phases predominated, having an important role in attenuating the Sb release from the different types of mine waste; average Sb_2O_5 contents of 0.12–0.31 wt% were found in C-(A)-S-H phases.

1. Introduction

Antimony is a toxic trace element of increasing concern due to its wide distribution in the environment. Antimony has no known biological function (Filella et al., 2002) and can cause serious adverse effects to living organisms above certain threshold concentrations (Kabata--Pendias and Mukherjee, 2007). It can inhibit culturable soil bacteria and fungi (He et al., 2019), cause diverse harmful effects on Sb-intolerant plants (e.g., growth retardation, restricted uptake of certain essential elements, photosynthesis inhibition, and reduction in the synthesis of some metabolites) (Feng et al., 2013), and threaten animal and human health in different ways. In humans, chronic exposure by inhalation and/or oral ingestion can provoke diverse diseases, including respiratory affections (e.g., cough, chronic bronchitis, chronic emphysema, and pneumoconiosis), gastrointestinal problems, alterations in immune and cardiovascular functions, reproductive disorders, and likely lung cancer when Sb enters the body via inhalation (Saerens et al., 2019). It is considered a priority pollutant by the European Union (EU) and the United States Environmental Protection Agency (US EPA). Thus, drinking water standards for Sb have been set at 5, 6, and 20 μg L^{-1} by EU, US EPA, and World Health Organization (WHO), respectively. The maximum permissible Sb concentration in soils receiving sewage sludge

* Corresponding author. Department of Environmental Geochemistry, IRNASA (CSIC), C/ Cordel de Merinas 40-52, 37008, Salamanca, Spain.
E-mail address: esther.alvarez@irnasa.csic.es (E. Álvarez-Ayuso).

https://doi.org/10.1016/j.jclepro.2022.133671
Received 24 March 2022; Received in revised form 21 July 2022; Accepted 14 August 2022
Available online 19 August 2022

has been established by the WHO at 36 mg kg-^{1} (Chang et al., 2002). Additionally, in some European countries, guideline values for Sb in soils have been defined on the basis of different levels of risk (Carlon, 2007); values of 10 and 50 mg kg-^{1} for ecological and health risks (Ministry of the Environment, Finland, 2007), respectively, are considered a good approximation of different national soil guidelines (Tóth et al., 2016).

Antimony is emitted by natural geogenic processes and anthropogenic activities. Its main anthropogenic sources are mining operations, metallurgical processes, energy production from fossil fuels, pigment and ceramic/glass manufacture, road traffic, shooting practices, and waste incineration and disposal (He et al., 2019). Of them, mining and metallurgical activities are considered the major ones (Guo et al., 2014a). Antimony scarcely occurs as the native element because of its chalcophile character, thus readily forming sulfides either alone or with other chalcophile elements such as silver, copper, and lead (Alloway, 1995). Stibnite (Sb_2S_3) is the primary exploitable ore of Sb (Anderson, 2001). Thus, Sb is principally mined from quartz-stibnite vein deposits of hydrothermal origin (Schwarz-Schampera, 2014). The exploitation of these deposits, including mining, beneficiation, and smelting processes, has provoked a serious environmental issue. This is especially significant at historic mine sites, where mine wastes have been usually exposed to atmospheric conditions without a proper management, releasing Sb and impacting adversely the surrounding environment (Bolan et al., 2022). Thus, in these scenarios the Sb contents in soils and waters can result greatly increased, attaining levels above 1000 times the typical Sb contents in uncontaminated soils and fresh waters [$<$ 10 mg kg^{-1} (Wilson et al., 2010) and $<$1 μg L^{-1} (Filella et al., 2002), respectively].

Stibnite readily oxidizes under atmospheric conditions within short periods of time (Ashley et al., 2003), excluding highly reducing environments (Vink, 1996). Moreover, this process is catalyzed under acid conditions in the presence of ferric ion and under mild basic conditions in the presence of basic cations (Biver and Shotyk, 2012). The oxidation of stibnite gives rise to diverse weathering products that can partially attenuate the release of Sb into the environment. Stibnite weathering products include soluble antimonates and antimony sulfates, oxides of different solubility and stability [senarmontite (α-Sb_2O_3), valentinite (β-Sb_2O_3), cervantite (α-Sb_2O_4), and stibiconite [$Sb_3O_6(OH)$], and sparingly soluble phases such as minerals of the roméite group ($Ca_2Sb_2O_7$) and iron antimonates [mostly schafarzikite ($FeSb_2O_4$) and tripuhyite ($FeSbO_4$)] (Roper et al., 2012). Additionally, in mine settings where iron sulfides co-occur with stibnite, other phases can also act as important sinks of Sb. These are Fe (oxyhydr)oxides [mostly hydrous ferric oxides (Flaková et al., 2017) and goethite (α-FeOOH) (Borčinová Radková et al., 2020)] and iron hydroxy sulfates such as jarosite [$KFe_3(SO_4)_2(OH)_6$] (Courtin-Nomade et al., 2012) and schwertmannite [$Fe_{16}O_{16}(OH)_{12}(SO_4)_2$] (Manaka et al., 2007). Despite the Sb attenuation capacity of weathering products of stibnite and iron sulfides, the different types of waste resulting from the exploitation of stibnite ore deposits are reportedly classified as hazardous and toxic materials because of their leachable Sb contents [smelting waste (Salihoglu, 2014), mine waste rocks (Cappuyns et al., 2021), and mine tailings (Álvarez-Ayuso et al., 2022)]. Therefore, measures should be adopted to avoid or restrict the off-side migration of this toxic element and its negative effects on affected ecosystems.

Different stabilization and encapsulation techniques have been investigated to deal with mine wastes, including establishment of surface covers, amendment treatments, solidification processes by cementation or geopolymerization, and development of protective coatings (Álvarez-Ayuso, 2022). The technique based on surface covers appears unsuitable to treat mine wastes derived from the exploitation of stibnite ore deposits. Ideally, surface covers avoid the oxidant access, leading to the establishment of reducing conditions that prevent sulfide oxidation. Nevertheless, the rapid stibnite dissolution process and the early co-occurrence of weathering products hamper the effective application of this strategy (Álvarez-Ayuso, 2022). The researches on the passivation of Sb-bearing mine waste by means of protective coatings have been focused on the development of phosphate covering layers (Harris and Lottermoser, 2006), but attempts to create such coatings on Sb sulfides failed. This unsuccessful performance was ascribed to the lack of iron in the lattice of target minerals, thus preventing the formation of iron phosphate (Harris and Lottermoser, 2006). Some stabilization systems based on the application of different amendments have been proposed, including phosphate materials (Munksgaard and Lottermoser, 2013), biochar (Gu et al., 2020), and reactive magnesia (Zhang et al., 2022). The impact of these treatments on the mobility of Sb in mine wastes was quite dissimilar. The application of phosphate materials and biochar showed a negative effect, increasing the release of Sb as a result of phosphate competition with Sb for adsorption sites (Munksgaard and Lottermoser, 2013; Gu et al., 2020), whereas the incorporation of reactive magnesia decreased considerably the leachability of Sb through its retention by newly formed hydrated gels (Zhang et al., 2022). Once proved the effectiveness of a particular amendment treatment, one of the main constraints of this technique is the amendment application to mine wastes that have already been dumped (Lottermoser, 2010). A thorough mixing of amendment and mine waste is required; thus, its right effective application is only possible when mine waste is being dumped. Of solidification processes, geopolymerization has been found ineffective to deal with Sb-bearing mine waste. Particularly, the Sb waste slag from the thermal processing of Sb ore was subjected to geopolymerization using the usual alkaline activators [sodium silicate (NaSil)/NaOH solutions] to promote this process (Salihoglu, 2014). Derived geopolymers showed increased Sb releases as compared to untreated wastes. This behavior was attributed to the relatively higher solubilities of compounds that oxyanions form with alkaline elements (Salihoglu, 2014). Therefore, cementation gathers some significant advantages. It is an affordable technique—materials used as binders (cement, slaked lime, pozzolanic by-products, and so forth) are low-cost and readily available—, has proven its effectiveness to treat mine wastes containing As—a metalloid with similar geochemical behavior to Sb—, and derived products could be employed as fill materials; particularly, they can find their way as a geotechnical support in underground mining operations, thus reducing surface storage requirements and restoration costs (Yilmaz et al., 2014). Also, the use of mine wastes as substitutes for natural aggregates in concrete in some civil engineering applications has been proposed (Park et al., 2019), thus preserving natural resources and representing a sustainable way of dealing with them. Anyway, such recycling approach requires an effective encapsulation of mine wastes to hinder or greatly minimize the toxic element release. In spite of the promising potential of this technique to treat Sb-bearing mine wastes, the studies performed in this regard are really scarce (Salihoglu, 2014; Gao et al., 2020). Moreover, these studies have been mainly focused on mine wastes with low total Sb contents ($<$0.2%) (Gao et al., 2020). Concerning specifically wastes derived from the exploitation of Sb ore deposits, so far only basic smelting wastes have been evaluated (Salihoglu, 2014). Furthermore, in this case only high binder proportions (75 wt%) were employed in the encapsulation processes, thus importantly increasing the final generated amounts of encapsulated waste. More research is needed to establish the feasibility of the cementation technique to mitigate the risks posed by the different Sb mine wastes and the suitable options to further handle the derived cemented materials.

The main objective of this study was to assess the use of cement encapsulation processes to deal with different types of waste generated from the exploitation of stibnite ore deposits, namely, mine waste rocks, mine tailings, and smelting waste, studying the following aspects: a) structural stability of encapsulated materials b) leaching behavior of Sb in solidified mine wastes by means of different leaching tests, and c) mineralogical and chemical characteristics of encapsulated materials.

2. Materials and Methods

2.1. Mine wastes

Mine waste rocks, mine tailings, and smelting waste resulting from the San Antonio mine, which exploited the most important stibnite ore deposit in Spain, were employed in the cement encapsulation processes. This deposit is located approximately 10 km southwest of the village of Albuquerque in the northwest of the province of Badajoz. It is a hydrothermal strata-bound deposit, although mineralized bodies also appear in veins. The mineralization is embedded in a calcareous belt of black limestones, calcareous shales, and intraformational breccias and in some siliceous layers of Devonian age. The main mineral association is mostly composed of quartz–stibnite–scheelite ($CaWO_4$), although berthierite ($FeSb_2S_4$) and pyrite (FeS_2) are also present in the ore body, together with arsenopyrite (FeAsS) and antimony as accessories (Gumiel and Arribas, 1987). This deposit was exploited from 1940 to 1986. Mining, mineral processing, and metallurgical operations produced important amounts of wastes. Mine waste rocks (up to centimetric size) were accumulated in dumps and mine tailings and smelting waste were deposited on the land, being exposed to the atmosphere, thus experiencing years of weathering with the consequent pollution of the surrounding environment (Álvarez-Ayuso et al., 2013). The volume of mine waste has been estimated to be approximately 3 t (Murciego et al., 2007).

The climate in this area is classified as Csa by the Köppen-Geiger system. This is a Mediterranean climate with hot summers. Particularly, this area has a warm temperate climate, with the winter season being much rainier than the summer season. Its annual average temperature and rainfall are 16.3 °C and 656 mm, respectively. During the year, the temperature generally varies between 2 °C and 33 °C, rarely decreasing below −3 °C or increasing above 38 °C. In the warm period (from mid-June to mid-September) the average maximum temperature is 29 °C and in the cold period (from mid-November to early March) the average maximum temperature reaches 16 °C. The driest months are July and August, where monthly average precipitation stays below 10 mm, whereas in the rainiest time (October–December) the monthly average precipitation attains a value of 79 mm.

Mine waste rocks, mine tailings, and smelting waste considered in this study are classified as toxic and hazardous according to their Sb leaching behavior as determined the European leaching test EN-12457-4 (2002) and the toxicity characteristic leaching procedure (TCLP) (Álvarez-Ayuso et al., 2022). Their main Sb-bearing phases are Fe (oxyhydr)oxides and/or mixtures of Fe and Sb (oxyhydr)oxides; also, natrojarosite [$NaFe_3(SO_4)_2(OH)_6$] and tripuhyite occur in the smelting waste (Álvarez-Ayuso et al., 2022). The mineralogical composition of mine waste rocks and mine tailings consists primarily of silicate minerals and carbonate minerals, with the former being more abundant in mine waste rocks and the latter dominating in mine tailings. The smelting waste has a more diverse mineralogical composition [iron hydroxy sulfates, silicate minerals, calcium sulfates, iron (oxyhydr)oxides, and Sb minerals], where natrojarosite is the mineral most abundant. Although the smelting waste has the highest total Sb content, mine waste rocks and mine tailings show greater leachable Sb levels as a result of their lower content in Sb-scavenging minerals/phases (Álvarez-Ayuso et al., 2022). The mine waste rocks and mine tailings have an alkaline character and the smelting waste is acidic (Álvarez-Ayuso et al., 2022). The specific characteristic of the three types of mine waste (mineralogical and chemical composition, leachable Sb levels, and pH of leachates) are given in Table 1.

Table 1
Characteristics of mine wastes.

	Mine waste rocks	Mine tailings	Smelting waste
	Mineralogical composition (%)		
	Quartz (52.3 ± 0.4) Muscovite (28 ± 1) Dolomite (6.0 ± 0.3) Calcite (5.4 ± 0.4) Clinochlore (4.5 ± 0.3) Microcline (1.9 ± 0.2) Kaolinite (1.7 ± 0.2)	Quartz (51.6 ± 0.3) Calcite (31.7 ± 0.4) Dolomite (8.4 ± 0.5) Muscovite (8.4 ± 0.3)	Natrojarosite (45.0 ± 0.5) Quartz (19.7 ± 0.3) Gypsum (16.8 ± 0.2) Hematite (8 ± 1) Biotite (6 ± 1) Goethite (3.5 ± 0.2) Gudmundite (1.2 ± 0.1) Stibiconite (0.51 ± 0.06)
	Chemical composition (%)		
Sb_2O_5	0.720 ± 0.012	0.145 ± 0.004	6.26 ± 0.06
Al_2O_3	12.5 ± 0.9	3.30 ± 0.11	3.29 ± 0.07
CaO	9.06 ± 0.06	21.6 ± 0.7	4.21 ± 0.17
Fe_2O_3	3.68 ± 0.04	1.74 ± 0.03	35.3 ± 0.9
K_2O	3.51 ± 0.16	0.985 ± 0.014	1.02 ± 0.02
MgO	1.56 ± 0.06	1.11 ± 0.06	0.058 ± 0.006
MnO_2	0.168 ± 0.003	0.138 ± 0.007	0.051 ± 0.002
Na_2O	1.39 ± 0.06	1.11 ± 0.02	3.17 ± 0.16
P_2O_5	0.266 ± 0.043	0.228 ± 0.035	0.335 ± 0.012
SO_3	0.519 ± 0.031	0.148 ± 0.014	24.7 ± 0.1
SiO_2	49.6 ± 0.6	40.1 ± 2.3	15.3 ± 1.6
	Leached Sb concentrations (mg L^{-1}) (TCLP)		
	6.86 ± 0.94	2.02 ± 0.28	1.05 ± 0.12
	Leachable Sb contents (mg kg^{-1}) (EN-12457, 2002)		
	28.4 ± 2.6	13.7 ± 0.6	1.05 ± 0.17
	pH of leachates (EN-12457, 2002)		
	7.58 ± 0.11	7.67 ± 0.50	4.35 ± 0.13

[Notes: Chemical composition determined by acid digestion according to the method of García-Sanchez and Saavedra-Alonso (1983)].

2.2. Cement encapsulation processes

The materials used as binders in the encapsulation processes were ordinary Portland cement (OPC) CEM I 52.5 R and calcium hydroxide (Cementos Tudela Veguín). Their pH, as determined by the water-saturated paste method, is 13.0 and 12.8, respectively. Their mineralogical characterization was performed by powder X-ray diffraction (XRD) on a D8 Advance Bruker diffractometer (Bruker Corporation, Billerica, Massachusetts, USA) using the Cu Kα radiation. The mineralogical composition of OPC is mainly integrated by haturite (Ca_3SiO_5), gismondine ($CaAl_2Si_2O_8{\cdot}4H_2O$), and larnite ($Ca_2SiO_4$), together with browmillerite (Ca_2FeAlO_5) and anhydrite ($CaSO_4$); the occurrence of low amounts of calcite ($CaCO_3$), dolomite [$CaMg(CaCO_3)$], gypsum ($CaSO_4{\cdot}2H_2O$), and quartz was also identified. Calcium hydroxide consists mostly of portlandite [$Ca(OH)_2$], although calcite, anhydrite, and quartz were also detected. Their chemical composition was determined by acid digestion following the method of García-Sánchez and Saavedra-Alonso (1983). Accordingly, OPC presents the following chemical composition: Al_2O_3: 5.11%, CaO: 67.5%, Fe_2O_3: 2.86%, K_2O: 1.18%, MgO: 3.34%, MnO_2: 0.08%, Na_2O: 1.07%, P_2O_5: 0.43%, SO_3: 6.48%, and SiO_2: 11.9%; and that of calcium hydroxide is as follows: Al_2O_3: 0.14%, CaO: 74.9%, Fe_2O_3: 0.15%, K_2O: 0.25%, MgO: 0.35%, MnO_2: 0.04%, Na_2O: 1.04%, P_2O_5: 0.29%, SO_3: 1.71%, and SiO_2: 1.92%. Different OPC:calcium hydroxide mixtures were employed [A = 100:0 wt%, B = 90:10 wt%, C = 80:20 wt%, and D = 60:40 wt%]. The different types of Sb-bearing mine waste [all of them at particle size < 5 mm in order to clearly fulfil the minimum ratio (3:1) between the diameter of monolith specimens and the maximum coarse aggregate size required by the Unconfined Compressive Strength (UCS) test] were mixed separately with the indicated binder mixtures using binder proportions of 10, 20, 40, 60, and 80 wt%. Then, deionized water was incorporated slowly to the homogeneous solid mixtures to reach a water content [water/(mine waste + binder + water)] of 15–35%, with the amount of water

increasing within this range with the increasing binder content. Pastes were thoroughly mixed for 5–10 min to complete homogenization. Afterwards, the different pastes were cast in triplicate in ø30 mm × 60 mm polypropylene cylinders, sealed, and cured at room temperature (22 °C ± 2 °C) for 28 days. After curing, the samples were removed from the molds to their characterization.

2.3. Mechanical behavior

The mechanical behavior of derived solidified mine wastes was assessed in order to determine their suitability to endure the compressive stress generated under the usual overburden pressures in landfills, their appropriateness to satisfy the compressive strength requirements for fill materials, and to know the possible concrete type applications to which they could be aimed as regards their developed strengths. The mechanical behavior of the monolith samples was evaluated using the UCS test. It was conducted in compliance with the standards EN-12504-1 (2020) and EN-12390-3 (2020). A Toni Technik compressive strength testing apparatus (Toni Technik Baustoffprüfsysteme GmbH, Berlin, Germany) was employed. Measurements were performed on three replicates of each monolith sample derived from the different encapsulation conditions applied to the three types of Sb-bearing mine waste subject of study.

2.4. Leaching behavior

Different tests were conducted on the encapsulated wastes to determine the leaching behavior of Sb: the European leaching test EN-12457-4 (2002), the TCLP, and the tank leaching test. The European leaching test EN-12457-4 (2002) was applied to all the materials derived from the encapsulation processes. Following this test, crushed materials (<10 mm) were subjected in triplicate to a shaking period for 24 h by means of a rotary shaker at 10 rpm using deionized water as extractant and a liquid/solid (L/S) ratio of 10 L kg^{-1}. After sedimentation and filtration through 0.45 μm filters, the extracts were analyzed for Sb by inductively coupled plasma atomic emission spectrometry (ICP-AES) employing a Varian 720-ES apparatus (Varian, Inc., Agilent Technologies, Santa Clara, California, USA). When the Sb concentrations were below the ICP-AES detection limit (0.1 mg L^{-1}) analyses were performed by Electrothermal Atomic Absorption Spectrometry (ETAAS), employing a Varian Spectra AA-220 apparatus equipped with a GTA 110 graphite atomizer (Varian, Inc., Agilent Technologies, Santa Clara, California, USA). The TCLP was also applied to all the materials derived from the encapsulation processes. According to this test, crushed materials (<9.5 mm) were subjected in triplicate to a shaking period for 18 h by means of a rotary shaker at 30 rpm using buffered acetic acid as extractant and a L/S ratio of 20 L kg^{-1}. Following sedimentation and 0.45 μm filtration, the extracts were analyzed for Sb by ICP-AES or ETAAS depending on the Sb concentration level (above or below 0.1 mg L^{-1}, respectively). The tank leaching test was performed on monolithic samples following the NEN-7375 (2004) procedure. Monolithic specimens of ø 42 mm × 50 mm fulfilling the leaching test requirements regarding the test piece dimensions were employed. Monolithic samples derived from the encapsulation processes using binder proportions of 10, 20, and 40 wt% were subjected to this test. In compliance with it, monolithic specimens underwent in triplicate a leaching process performed in eight stages in a closed tank using deionized water as extractant at a volume equal to 5 times the volume of the test piece. The extractant was drained and replenished at certain time intervals (0.25, 1, 2.25, 4, 9, 16, 36, and 64 days) established specifically by the NEN-7375 (2004) procedure. The extracts obtained at the different leaching periods were analyzed for Sb by ICP-AES or ETAAS depending on the Sb concentration level and for pH and electrical conductivity (EC). The pH was determined potentiometrically and the EC was analyzed conductometrically using for such measurements a Fisher Scientific Accumet AB200 pH/conductivity meter (Fisher Scientific, Thermo Fisher Scientific, Waltham, Massachusetts, USA).

2.5. Mineralogical and chemical characterization

Previously to perform the leaching tests, the mineralogical characterization of the encapsulated materials was carried out by XRD and scanning electron microscopy (SEM). Analyses by XRD were performed on the materials derived from the encapsulation processes using binder proportions of 10, 20, and 40 wt%. Unoriented finely ground samples were analyzed by the aforementioned diffractometter using also the Cu Kα radiation. Samples were scanned from 3° to 80° 2θ. Scanning electron microscopy analyses were carried out on materials derived from the encapsulation processes using binder proportions of 40 wt% and OPC: calcium hydroxide mixtures of 100:0 and 90:10 wt%. Test pieces coated with gold were observed by a SEM JEOL-6610LV scanning electron microscope (JEOL Ltd., Tokyo, Japan) equipped with a tungsten filament electron beam source and coupled to an energy dispersive X-ray (EDX) spectrometer INCA Energy 350–Xmax 50 (Oxford instruments) for semi-quantitative chemical analysis and element distribution maps. Images were recorded in backscattered electron (BSE) mode at an accelerating voltage of 20 kV. The following elements were analyzed by EDX: Sb, S, Fe, Ca, K, Na, Si, Al, Mg, O, and C. Additionally, spot chemical analyses on possible Sb carrier phases were performed by electron microprobe analysis (EMPA). Carbon-coated polished thin sections of waste samples embedded in resin were analyzed by wavelength-dispersive spectrometry (WDS) using a JEOL Superprobe JXA-8900M electron probe microanalyzer (JEOL Ltd., Tokyo, Japan) at CNME using an accelerating voltage of 15 kV. The analyzed elements were Sb, S, Fe, Ca, K, Na, Si, Al, and Mg.

3. Results and discussion

3.1. Mechanical behavior

The compressive strength development of the encapsulated wastes after 28 days of curing using different binder and OPC:calcium hydroxide proportions are shown in Fig. 1. The UCS values increased gradually as the binder content in the solidified wastes was increased. At the lowest binder:mine waste ratios (10:90 and 20:80 wt%), the encapsulated wastes generated from mine tailings developed the lowest compressive strengths. The materials derived from the three types of waste showed to decrease their UCS values as the calcium hydroxide content increased in the binder mixture. In any case, all encapsulated wastes developed compressive strengths higher than that considered appropriate to keep their physical integrity under the common overburden pressures in landfills (0.35 MPa) (Choi et al., 2009), with values within the ranges of 1.4–45.3, 0.8–38.2, and 0.9–45.6 MPa for encapsulated wastes generated from mine waste rocks, mine tailings, and smelting waste, respectively. Hence, this criteria was met even at a relatively low binder:mine waste ratio (10:90 wt%), regardless of the employed binder mixture, thus minimizing the generated amounts of encapsulated waste. Additionally, all the generated materials fulfilled the compressive strength requirements for their use as fill materials (1 MPa) (Gao et al., 2020), except for those derived from mine tailings and smelting waste at the lowest binder:mine waste ratio (10:90 wt%) using the highest calcium hydroxide content in the binder mixture (40 wt%). Materials prepared using low binder proportions are usually those intended for backfill in mines. The mechanical behavior of such materials has been found to differ when backfilling (Yilmaz et al., 2014). Anyway, the UCS of in situ backfill has shown to be generally 2–4-fold those derived at laboratory scale (Yilmaz et al., 2014).

3.2. Leaching behavior

3.2.1. Batch shaking leaching tests

The leaching characteristics of the encapsulated wastes determined

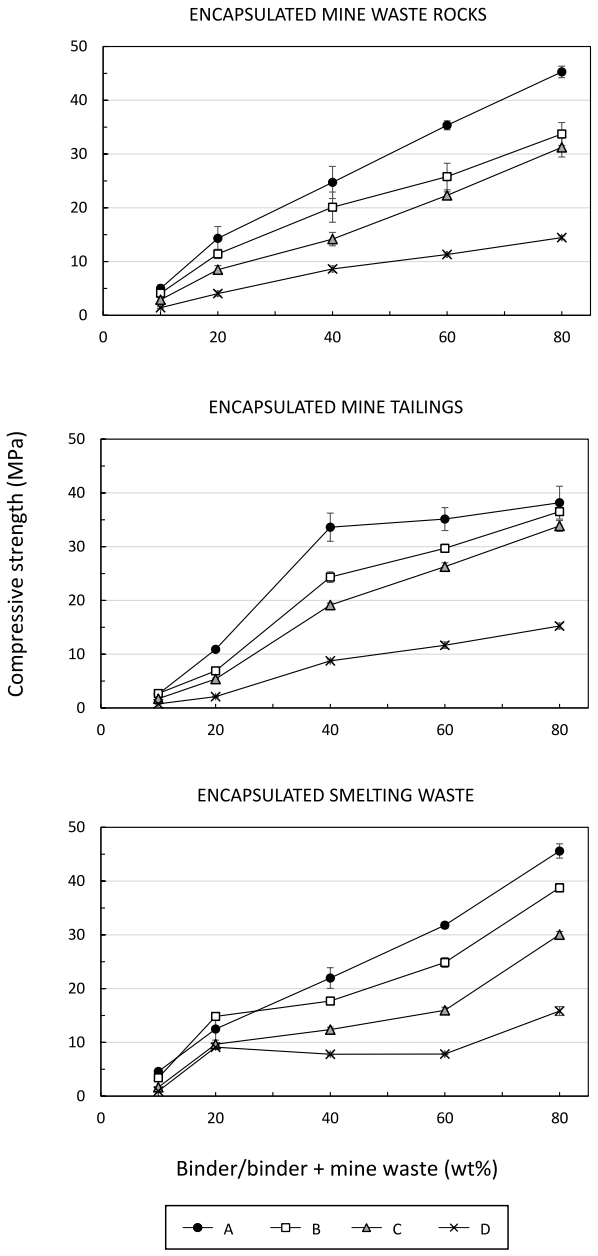

Fig. 1. Compressive strength development of encapsulated mine wastes using different binder:mine waste ratios and different calcium hydroxide amounts in the binder mixture (A: 0 wt%, B: 10 wt%, C: 20 wt%, and D: 40 wt%).

following the applied batch shaking leaching tests [EN-12457-4 (2002) and TCLP] are indicated in Fig. 2.

According to the European leaching test EN-12457-4 (2002), the leachable Sb contents in the encapsulated materials derived from mine waste rocks and mine tailings decreased importantly at the different binder and OPC:calcium hydroxide proportions with respect to those in the untreated wastes, from 28.4 to < 3 mg kg^{-1} and from 13.7 to < 0.6 mg kg^{-1}, respectively. The leachable Sb content limit established by the Council Decision 2003/33/EC (European Council Decision, 2003) for acceptance at landfills for non-hazardous materials (0.7 mg kg^{-1}) was fulfilled at any tested conditions for the encapsulated mine tailings. Nevertheless, this limit was not accomplished for the encapsulated mine waste rocks at the lowest binder:mine waste ratios (10:90 and 20:80 wt %). The incorporation of calcium hydroxide in the binder mixture to encapsulate both types of mine waste showed a positive effect at low binder:mine waste ratios (especially at 10:90 wt%) and at low amounts of calcium hydroxide in the binder mixture (10 wt%). At these conditions, the leachable Sb content in the encapsulated mine waste rocks and mine tailings was decreased by 43 and 53% with respect to those where only OPC was employed as binder. In contrast to what happened with mine waste rocks and mine tailings, the cementation processes caused a negative impact on the leachable Sb content of the smelting waste when low binder:mine waste ratios (10:90 and 20:80 wt%) were employed. Thus, the leachable Sb contents in the derived encapsulated materials increased importantly with respect to that in the untreated smelting waste, from 1.05 up to 21.5 and 2.05 mg kg^{-1}, respectively. At higher binder proportions, the leachable Sb content decreased down to that of the untreated smelting waste and that required for acceptance at landfills for non-hazardous materials (0.7 mg kg^{-1}). At such conditions, the incorporation of calcium hydroxide in the binder mixture did not show a significant effect on the leachable Sb content of generated materials.

According to the TCLP, the cementation processes of mine waste rocks and mine tailings performed using the lowest binder:mine waste ratio (10:90 wt%) did not attenuate in general the Sb leaching from them, resulting even enhanced in some instances. As the binder:mine waste ratio increased the Sb concentrations released from the encapsulated mine waste rocks and mine tailings decreased progressively, releasing much lower Sb concentrations than the untreated wastes (from 6.86 to < 1.7 mg L^{-1} and from 2.02 to < 0.12 mg L^{-1}, respectively). Furthermore, at binder:mine waste ratios of 20:80 wt% and higher, almost all released concentrations were below the limit (0.6 mg L^{-1}) for the characterization of wastes as toxic, which was established at 100 times the US EPA drinking water standard (Guo et al., 2014a). According to the TCLP, the cementation processes of the smelting waste performed using low binder:mine waste ratios (10:90 and 20:80 wt%) did not perform well, increasing the Sb leaching with respect to that from the untreated waste (from 1.05 up to 11.5 mg L^{-1}). Nevertheless, at higher binder:mine waste ratios, the Sb leaching was importantly attenuated, with released Sb concentrations (<0.5 mg L^{-1}) staying below that from the untreated waste and the limit for the characterization of wastes as toxic.

3.2.2. *Tank leaching test*

The variation of cumulative leached Sb amounts from the encapsulated wastes with increasing time as derived from the tank leaching test is shown in Fig. 3 and the corresponding leachate pH values are indicated in Fig. 4.

The cumulative Sb amounts leached all along the leaching period from the encapsulated mine waste rocks at the lowest binder:mine waste ratio (10:90 wt%) using only OPC in the binder mixture reached a value of 45.3 mg m^{-2}. A progressive Sb leaching reduction was observed as the binder:mine waste ratio increased, decreasing down to 20.9 mg m^{-2} when a binder:mine waste ratio of 40:60 wt% was employed. The incorporation of calcium hydroxide in the binder mixture did not have a remarkable effect on Sb leaching, either in the leached amounts, which stayed more or less at similar values, or in the leaching tendency. In general, cumulative leaching curves showed an attenuated trend, especially those corresponding to the encapsulated mine waste rocks derived using a binder:mine waste ratio of 40:60 wt%. In the case of the encapsulated mine tailings, the increasing binder:mine waste ratio caused a less marked decrease in Sb leaching. The cumulative Sb amounts leached all along the leaching period from the encapsulated mine tailings at the lowest binder:mine waste ratio (10:90 wt%) showed values of approximately 13–16 mg m^{-2}. The cumulative leached amounts of Sb decreased down to approximately 8 mg m^{-2} when a binder:mine waste ratio of 40:60 wt% was employed, with decreases being only noticeable at some binder mixtures. The release of Sb was the highest from the encapsulated smelting waste. In this case, when using the lowest binder:mine waste ratio (10:90 wt%) in the encapsulation process, the cumulative Sb amounts leached all along the leaching period attained values in the range of 271–161 mg m^{-2}, decreasing

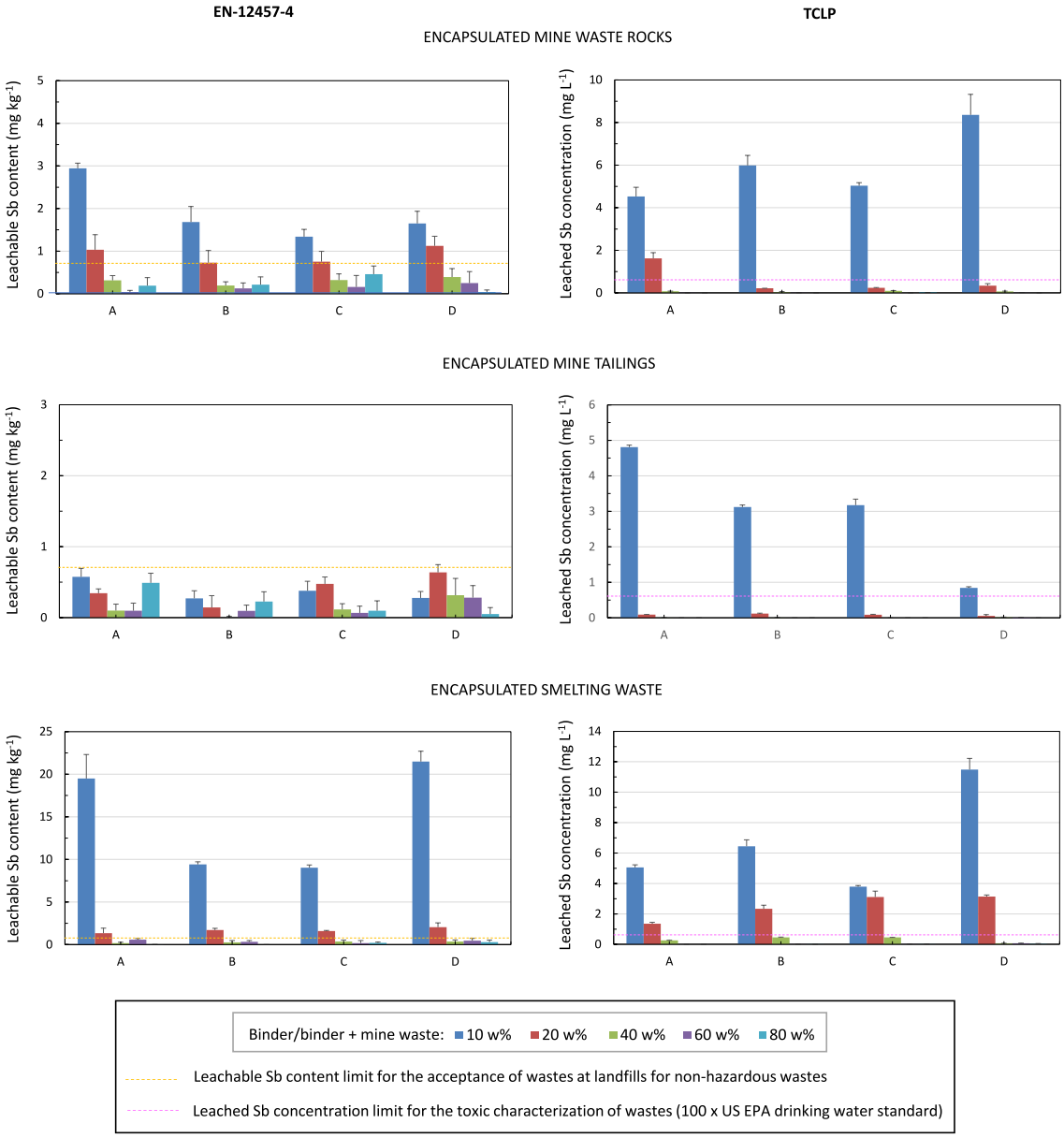

Fig. 2. Antimony leaching [EN-12457-4 (2002) and TCLP tests] from encapsulated mine wastes using different binder:mine waste ratios and different calcium hydroxide amounts in the binder mixture (A: 0 wt%, B: 10 wt%, C: 20 wt%, and D: 40 wt%).

within this range with the incorporation of calcium hydroxide in the binder mixture. In any case, a drastic reduction in the leaching of Sb was produced as the binder:mine waste ratio increased. Thus, the cumulative released amounts of Sb decreased down to 48.5–20.4 mg m^{-2} when a binder:mine waste ratio of 40:60 wt% was employed, representing decreases of approximately 80–90%. Moreover, at this ratio, the cumulative leaching curves tended to almost reach a steady state. In general, the lowest Sb releases took place from mine waste rocks and smelting waste encapsulated using a binder:mine waste ratio of 40:60 wt% and from mine tailings encapsulated using binder:mine waste ratios of 40:60 and 20:80 wt%.

The leachate EC (data not shown) and pH values of samples showing the lowest Sb releases met the NEN-7375 (2004) requirements to characterize the leaching process. Accordingly, the slope obtained from the lineal regression of the log of derived cumulative leaching against the log of leaching time is employed to infer the mechanism controlling the leaching process. Low slope values (≤0.35) are considered indicative of surface wash-off processes, whereas high slope values (>0.65) are characteristic of dissolution reactions. Intermediate values are attributed to diffusion-controlled release and ideally should generate a straight-line. All the slope values corresponding to samples with the lowest released amounts of Sb (Table 2) were in the range of 0.37–0.63 (R^2 = 0.930–0.996), suggesting that in such cases the Sb leaching mechanism was mainly diffusion controlled. This mechanism agrees with that found from the release of Sb under different leachants (deionized water, acetic acid, and dilute sulfuric/nitric acid) from low Sb-containing mine tailings encapsulated using metallurgical slag-based binders (Gao et al., 2020).

When the leaching is diffusion controlled, the effective diffusion coefficient, D_e (m^2 s^{-1}), can be calculated using the following formula (NEN-7375, 2004): $D_e = (\varepsilon_{64}/2654\ \rho\ U_{available})^2\ f$, where ε_{64} (mg m^{-2}) is the derived cumulative leaching over 64 days, ρ (kg m^{-3}) is the density of the test piece, $U_{available}$ (mg kg^{-1}) is the leachable available content determined according to the maximum availability leaching test NEN 7371 (2004), and f is a factor equal to 1 s^{-1}. pD_e (-log D_e) values < 11.0 are indicative of high mobility, whereas pD_e values > 12.5 are

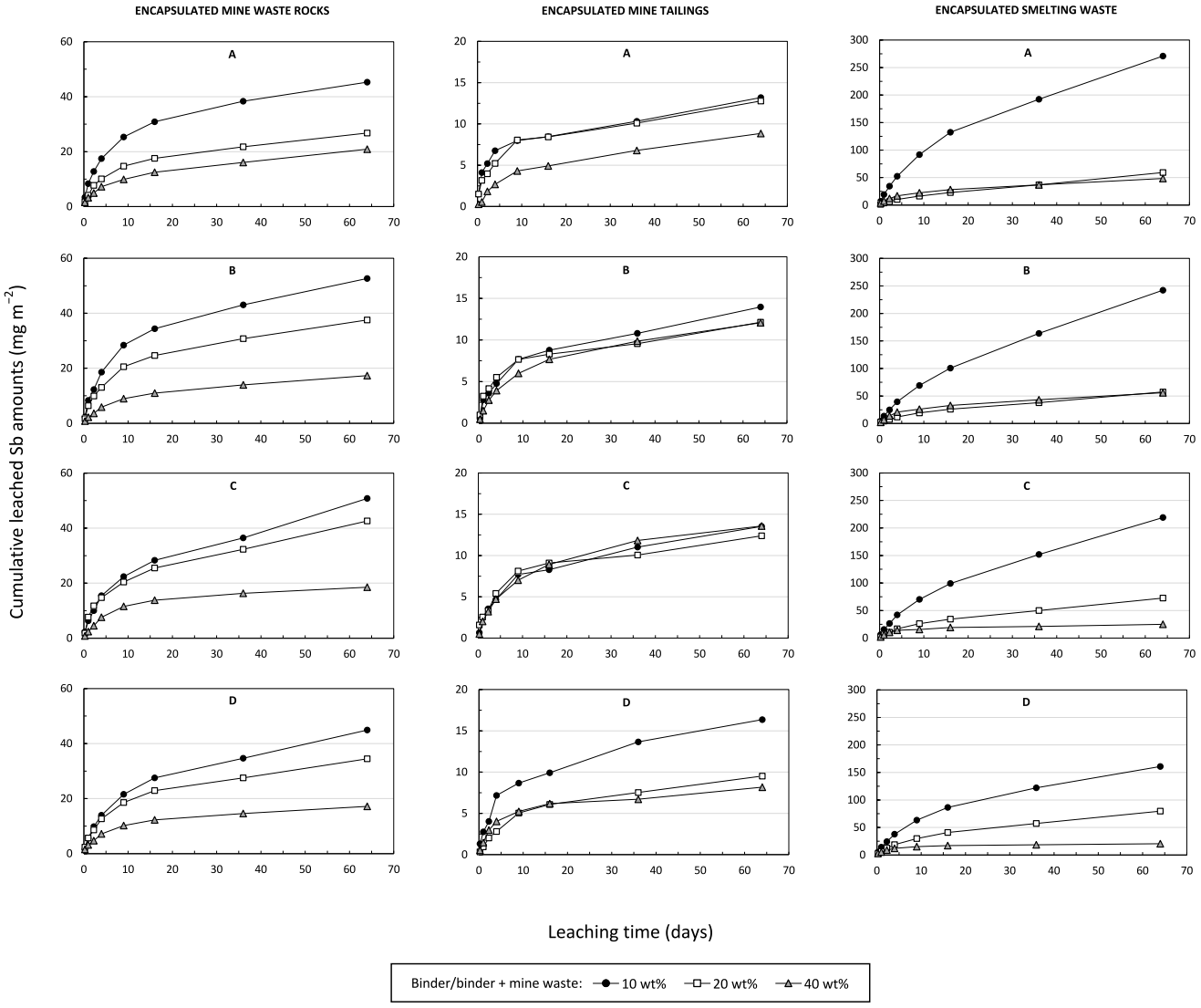

Fig. 3. Cumulative leached Sb amounts with increasing time (tank leaching test) from encapsulated mine wastes using different binder:mine waste ratios and different calcium hydroxide amounts in the binder mixture (A: 0 wt%, B: 10 wt%, C: 20 wt%, and D: 40 wt%).

characteristic of low mobile components. All the obtained pDe values (Table 2) were in the range of 13.2–15.2, indicating that the mobility of Sb from the encapsulated wastes was low and their suitability for disposal.

Some national legislations have been developed as regards secondary materials intended for application in the construction industry. In the Netherlands, the use of waste materials in the built sector is regulated by the Decree on Soil Quality (2007). Accordingly, the emission of parameters from molded building materials whose leaching is controlled by diffusion shall be determined by means of the leaching test NEN-7375 (2004). Under such conditions, the emission standard for recycling materials in open (un-insulated) construction applications is set at 8.7 mg Sb m^{-2}. This leaching limit is fulfilled by mine tailings encapsulated using some formulations with a binder:mine waste ratio of 40:60 wt%. Accordingly, such formulations could be employed in construction applications without the implementation of insulation, management, and control measures. In the case of mine waste rocks and smelting waste encapsulated using binder:mine waste ratios from 10:80 to 40:60 wt%, measures should be applied whereby virtually no contact occurs between the building material and water. Otherwise, formulations with lower contents in mine waste rocks and smelting waste should be employed in order to decrease the leaching of Sb below the emission requirement.

3.3. Mineralogical and chemical characterization

3.3.1. X-ray diffraction

The XRD patterns of the encapsulated mine wastes are shown in Fig. 5. The mineralogical composition of the encapsulated mine waste rocks included silicate minerals (quartz, muscovite, and chlorite) and carbonate minerals (calcite and dolomite), present originally in the untreated mine waste rocks, together with gypsum ($CaSO_4{\cdot}2H_2O$), portlandite, ettringite ($3CaO{\cdot}Al_2O_3{\cdot}3CaSO_4{\cdot}32H_2O$), and hydrocalumite [$Ca_4Al_2(OH)_{12}(OH)_2{\cdot}6H_2O$]. The three latter are compounds typically resulting from the hydration of OPC. Particularly, portlandite results from the OPC silicate hydration, whereas the hydration reactions between aluminates and gypsum lead to the formation of two different groups of phases called trisulfoaluminoferrite hydrates (AFt) and monosulfoaluminoferrite hydrates (AFm) (Aïtcin and Flatt, 2016.). Ettringite is the most important and representative phase within the AFt group and hydrocalumite is the OH-AFm group member. Portlandite was present in all the analyzed encapsulated mine waste rocks. Ettringite occurred in those derived using the highest calcium hydroxide content in the binder mixture (40 wt%), where it was present in small amounts.

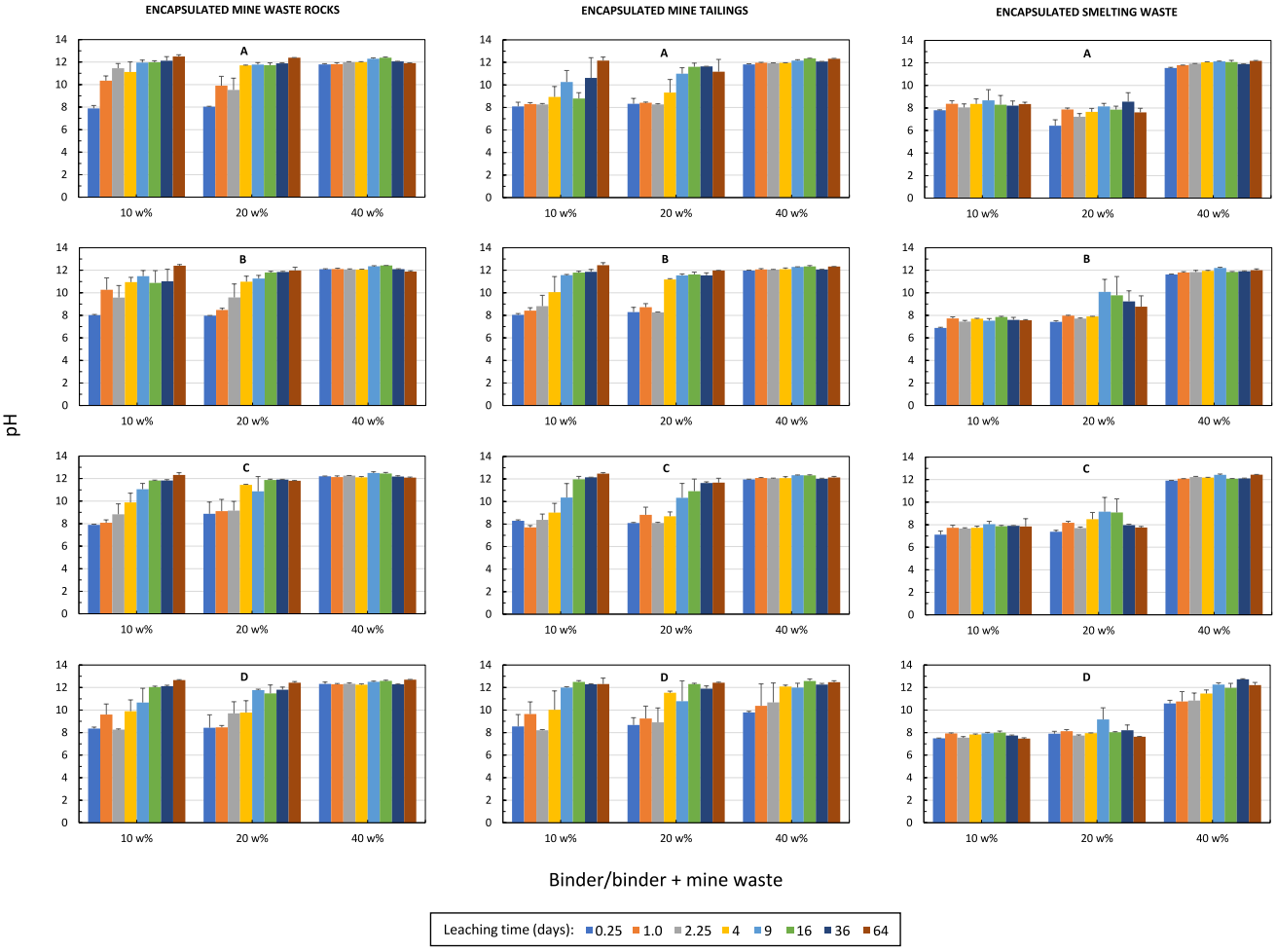

Fig. 4. pH of leachates with increasing time (tank leaching test) from encapsulated mine wastes using different binder:mine waste ratios and different calcium hydroxide amounts in the binder mixture (A: 0 wt%, B: 10 wt%, C: 20 wt%, and D: 40 wt%).

Hydrocalumite was only just appreciable in encapsulated mine waste rocks derived at a binder:mine waste ratio of 40:60 wt% when the highest calcium hydroxide content was employed in the binder mixture (40 wt%). In the case of encapsulated mine tailings, in addition to silicate minerals (quartz and muscovite) and carbonate minerals (calcite and dolomite), present originally in the untreated mine tailings, gypsum, portlandite, ettringite, and hydrocalumite also occurred in them. Portlandite and ettringite were present in all the analyzed encapsulated mine tailings and hydrocalumite in most of them. Ettringite occurred in small amounts and the presence of hydrocalumite was just perceptible. The minerals generated from the encapsulation processes of the smelting waste were ettringite and roméite. The amount of ettringite increased and that of roméite decreased as the binder content increased. All of these new formed minerals can act as Sb immobilizing agents. Antimonate adsorbs on portlandite and ettringite surfaces forming inner-sphere complexes (Cornelis et al., 2012a), showing intermediate affinity for portlandite and relatively low for ettringite (Cornelis et al., 2012a). Antimonate shows a strong affinity for AFm phases; the formation of a non-ideal solid solution has been suggested for the removal of antimonate by them (Cornelis et al., 2012a). In any case, roméite should be a more important Sb scavenger. However, roméite presents different structure depending on the solution composition (calcium concentration and pH) (Cornelis et al., 2011). The mineral structures having more calcium at higher pH show lower solubilities (Cornelis et al., 2012b). Accordingly, when roméite is the phase controlling the soluble Sb concentrations treatments that keep high calcium availability and pH have been proposed as suitable to decrease Sb release (Cornelis et al., 2012b). Anyway, roméite was practically absent in the encapsulated smelting waste derived at the suitable binder:mine waste ratio (40:60 wt%) to maintain low Sb leaching.

3.3.2. *Scanning electron microscopy*

Representative SEM-BSE images of encapsulated mine wastes focused on Sb-containing areas together with the corresponding element distribution maps are shown in Fig. 6.

The encapsulated mine waste rocks presented aluminosilicates, silicates, Fe (oxyhydr)oxides, Sb (oxyhydr)oxides, and some relicts of pyrite; all of them were embedded in a Ca-enriched matrix where calcite and C-(A)-S-H [calcium (aluminate) silicate hydrate] phases were detected. Antimony was mainly present as Sb (oxyhydr)oxides and associated with Fe (oxyhydr)oxides, although some occurrence in calcite and C-(A)-S-H was also inferred. Except for the occurrence of pyrite, the same phases were also found in the encapsulated mine tailings, with Fe (oxyhydr)oxides and mixtures of Fe and Sb (oxyhydr)oxides being also the main Sb carriers. In the encapsulated smelting waste, the occurrence of iron phases was really considerable, being the primarily scavengers of Sb. These included Fe (oxyhydr)oxides, mixtures of Fe and Sb (oxyhydr) oxides, and tripuhyite. In the encapsulating matrix, C-(A)-S-H compounds were identified.

The main Sb-bearing phases in the encapsulated mine wastes were the same as in the untreated mine wastes, except for natrojarosite in the smelting waste. This mineral was very abundant in the untreated smelting waste with an average Sb_2O_5 content of 1.43 wt% (Álvarez-Ayuso et al., 2022), whereas its occurrence in the encapsulated

Table 2
Mechanism controlling Sb leaching from encapsulated mine wastes (tank leaching test) as derived from the slope of log (derived cumulative leaching) vs log (leaching time) and effective diffusion coefficient values.

Encapsulated waste	Binder: mine waste ratio (wt %)	Ca $(OH)_2$/ Binder (wt%)	Slope	R^2	Mechanism	pD_e
Mine waste rocks	40:60	0	0.48 ± 0.01	0.995	Diffusion	14.0
		10	0.57 ± 0.03	0.984	Diffusion	14.5
		20	0.58 ± 0.04	0.966	Diffusion	14.7
		40	0.47 ± 0.02	0.988	Diffusion	13.2
Mine tailings	40:60	0	0.63 ± 0.04	0.977	Diffusion	14.5
		10	0.59 ± 0.04	0.979	Diffusion	13.9
		20	0.60 ± 0.04	0.971	Diffusion	13.9
		40	0.50 ± 0.05	0.946	Diffusion	14.1
	20:80	0	0.37 ± 0.02	0.979	Diffusion	14.5
		10	0.43 ± 0.04	0.952	Diffusion	14.1
		20	0.40 ± 0.02	0.981	Diffusion	14.1
		40	0.60 ± 0.03	0.980	Diffusion	14.5
Smelting waste	40:60	0	0.47 ± 0.01	0.996	Diffusion	14.0
		10	0.57 ± 0.04	0.973	Diffusion	14.3
		20	0.45 ± 0.05	0.930	Diffusion	15.0
		40	0.38 ± 0.03	0.958	Diffusion	15.2

smelting waste was really minor (except for materials derived using the lowest binder:mine waste ratios: 10:90 and 20:80 wt%), as revealed by XRD. Jarosite minerals are thermodynamically unstable (Ryu and Kim, 2022); their dissolution rates increase at low and high pH values [jarosite (Elwood Madden et al., 2012); natrojarosite (Zahrai et al., 2013); hazardous or toxic element-bearing jarosites (Islas et al., 2020)], with minimum dissolution rate values in the pH range of 3–4 for jarosite (Elwood Madden et al., 2012) and natrojarosite (Zahrai et al., 2013) and of 5–6 for hazardous jarosites (Islas et al., 2020). Above such pH values their dissolution takes place incongruently with the precipitation of Fe (oxyhydr)oxides which act as sinks of released Sb [at pH 7 (Karimian et al., 2017) and at pH 5.5 (Karimian et al., 2018)]. The oxyanions immobilized by jarosites have been found to importantly impact the mineral dissolution rates and transformation processes (Ryu and Kim, 2022). Oxyanions having smaller shared charge and forming stronger surface complexes with iron show slower mineral dissolution rates, more limited mineral transformation, and decreased releases (Ryu and Kim, 2022). The retention of antimonate by jarosite minerals takes place by incorporation into the mineral structure replacing octahedral Fe(III) (Courtin-Nomade et al., 2012). Antimonate has a relatively small shared charge (0.83), smaller than those of other oxyanions [arsenate (1.25) and selenite (1.33)] considered to have a relatively high affinity to the jarosite structure. Hence, a strong bond should be established between antimonate and jarosite minerals, as the smaller is the shared charge of the retained oxyanion the more strengthened results its bond with the jarosite structure (Ryu and Kim, 2022). In any case, the dissolution rates of jarosites increase progressively with the increasing pH from pH values at which dissolution rates are minimum [jarosite (Elwood Madden et al., 2012); natrojarosite (Zahrai et al., 2013); hazardous jarosites (Islas et al., 2020)]. Thus, considerable amounts of natrojarosite remained in the encapsulated smelting waste with leachate pH values of approximately 8 (those derived using the lowest binder:mine waste ratios: 10:90 and 20:80 wt%), whereas natrojarosite hardly persisted in the encapsulated smelting waste with leachate pH values of approximately 11–12 (those derived using a binder:mine waste ratio of 40:60 wt%).

Calcium (aluminate) silicate hydrate phases were mostly detected as binding agents in the matrix of cemented materials. These phases can also act as Sb immobilizing agents. Antimonate shows a strong affinity for C–S–H (calcium silicate hydrate) surfaces, much higher than for portlandite and ettringite (Cornelis et al., 2012a). Two different mechanisms have been proposed for the retention of antimonate by C–S–H surfaces; these are antimonate adsorption by deprotonated silanol groups via cation (Ca^{2+}) bridges, resulting in the formation of ternary complexes, and the formation of ions pairs between antimonate and calcium ions that are not adsorbed but accumulated really close to the C–S–H surface (Cornelis et al., 2012a). Other mechanisms suggested for the removal of different anions by C–S–H surfaces, such as ligand exchange of silanol hydroxyl groups (Bonhoure et al., 2003) and incorporation into the C–S–H structure replacing silicate (Tommaseo and Kersten, 2002), have been found not to occur in the removal of antimonate (Cornelis et al., 2012a).

3.3.3. *Electron microprobe analysis*

The spot chemical analyses performed on possible Sb-bearing phases in each type of encapsulated mine waste are indicated in Table 3. In the encapsulated mine waste rocks, Sb (oxyhydr)oxides showed the highest Sb content, with an average value of 51.13 wt% Sb_2O_5. Much lower average Sb_2O_5 contents were found in Fe (oxyhydr)oxide-enriched phases (3.26 wt%), aluminosilicates (3.04 wt%), silicates (0.35 wt%; 0.03 wt% in the specific case of quartz), calcite (0.20 wt%), and mixtures of calcite/portlandite (0.14 wt%). The Sb content in the main binding phase [C-(A)-S-H] reached values up to 0.24 wt% Sb_2O_5, with an average content of 0.13 wt% Sb_2O_5. In the encapsulated mine tailings, the highest Sb levels occurred in mixtures of Fe and Sb (oxyhydr)oxides, with an average value of 12.79 wt% Sb_2O_5. Likewise, lower average Sb_2O_5 contents were present in Fe (oxyhydr)oxides (1.31 wt%), aluminosilicates (1.28 wt%), silicates (quartz) (0.02 wt%), calcite (0.20 wt%), mixtures of calcite/portlandite (0.20 wt%), and C-(A)-S-H phases (0.12 wt%). In both types of encapsulated waste (mine waste rocks and mine tailings), the Sb levels present in carbonates and (alumino)silicates as well as in important Sb carriers [Fe (oxyhydr)oxides and mixtures of Fe and Sb (oxyhydr)oxides] were similar to those found in the untreated wastes (Álvarez-Ayuso et al., 2022), indicating that Sb was mostly preserved in the original Sb-bearing phases after the encapsulation process. It was found that the amount of Sb present in these mine wastes in desorbable forms was relatively little (<0.8% of the total Sb content) (Álvarez-Ayuso et al., 2022). Antimonate is structurally incorporated within Fe (oxyhydr)oxides by co-precipitation (Mitsunobu et al., 2010). Besides, over time, antimonate adsorbed on low-ordered hydrous Fe oxides results incorporated into their structure, probably by slow micropore diffusion and/or by replacement of surface octahedral Fe(III)

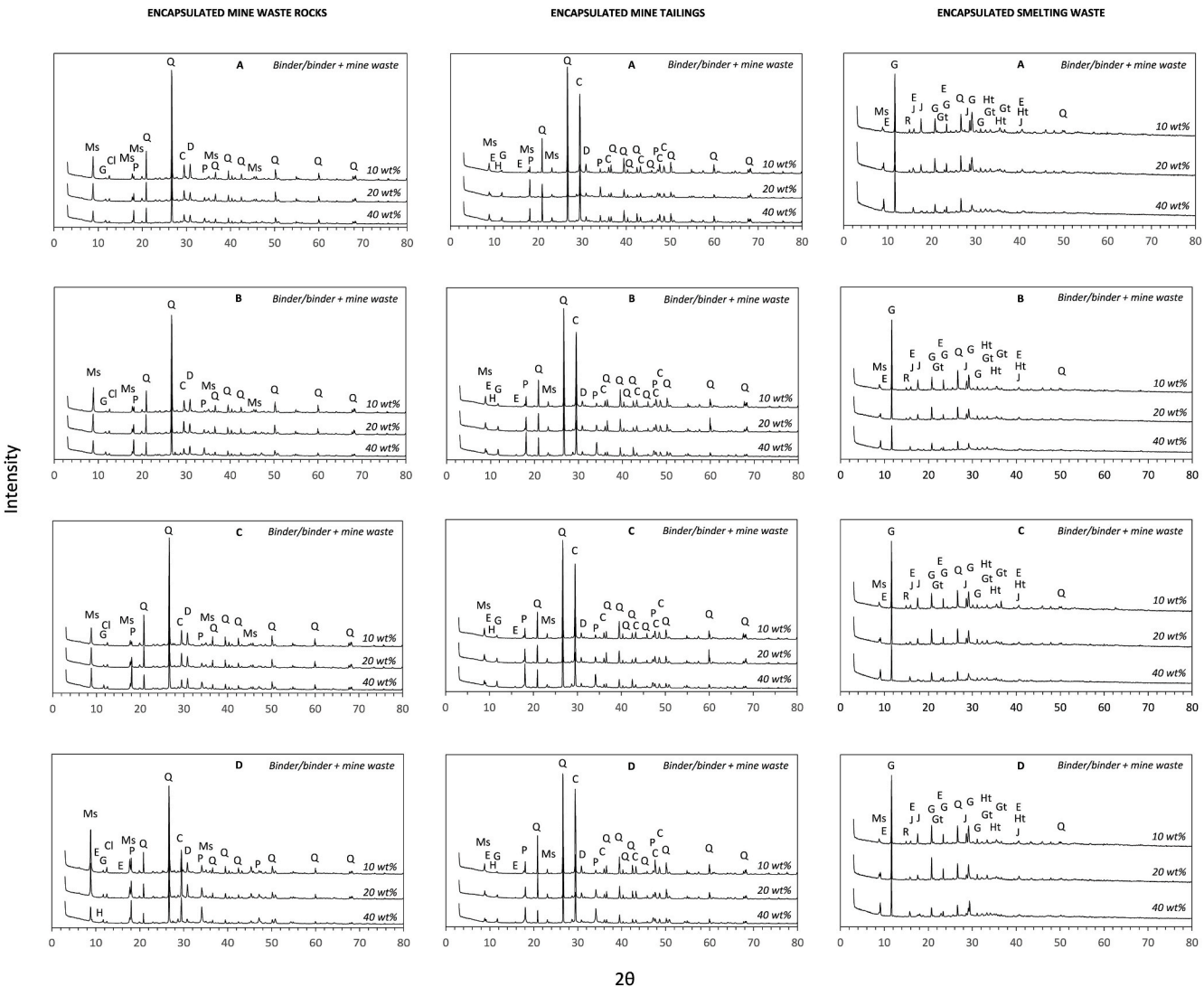

Fig. 5. XRD patterns of encapsulated mine wastes using different binder:mine waste ratios and different calcium hydroxide amounts in the binder mixture (A: 0 wt%, B: 10 wt%, C: 20 wt%, and D: 40 wt%). (C: calcite, Cl: chlorite, D: dolomite, E: ettringite, G: gypsum, Gt: Goethite, H: hydrocalumite, Ht: hematite, J: natrojarosite, Ms: muscovite, P: portlandite, Q: quartz, and R: roméite).

(Verbeeck et al., 2021). Contrary to elements adsorbed on solid surfaces, elements incorporated into solid structures are not importantly impacted by factors such as pH, ionic strength, and presence of competitive ions (Mitsunobu et al., 2010). Moreover, among the Sb (oxyhydr)oxides found in mining areas, stibiconite—the most frequent (Roper et al., 2012)—presents low solubility values (153.2–452.0 μg Sb L^{-1}) within a wide pH range (Biver and Shotyk, 2013).

In the encapsulated smelting waste important Sb levels were found in tripuhyite and in mixtures of Fe and Sb (oxyhydr)oxides with average Sb_2O_5 contents of 42.52 and 9.91 wt%, respectively. More moderate amounts of Sb were found in Fe (oxyhydr)oxides (up to 5.26 wt% Sb_2O_5), with an average value of 0.79 wt% Sb_2O_5 (0.05 wt% Sb_2O_5 in the case of hematite). The Sb content in C-(A)-S-H phases reached values of 0.44 wt% Sb_2O_5, showing an average value of 0.31 wt% Sb_2O_5. The Sb levels in Fe (oxyhydr)oxides and mixtures of Fe and Sb (oxyhydr)oxides present in the encapsulated smelting waste were decreased with respect to those found in the untreated waste (6.01 and 30.59 wt% Sb_2O_5 on average, respectively) (Álvarez-Ayuso et al., 2022). The increased precipitation of Fe (oxyhydr)oxides as a result of the dissolution of natrojarosite (especially at a binder:mine waste proportion of 40:60 wt%) should have decreased the overall contents of Sb in these phases. These freshly precipitated phases can scavenge the Sb released from natrojarosite dissolution. Additionally, C-(A)-S-H phases were involved in the attenuation of Sb in the encapsulation of the smelting waste, more than were in the encapsulation of the mine waste rocks/mine tailings. The Sb contents in C-(A)-S-H phases of the encapsulated smelting waste were approximately 2.5-fold those of the encapsulated mine waste rocks/mine tailings.

According to the mineralogical and chemical characterization, the cement encapsulation process of mine waste rocks and mine tailings preserved their main original Sb-bearing phases [Fe and Sb (oxyhydr) oxides] with similar Sb levels as those in untreated mine wastes. The pH raises provoked by cementation (up to 11.7–12.7) did not impact negatively on them, suggesting that Sb present in Fe (oxyhydr)oxides was mainly incorporated into their structure and the occurrence of Sb (oxyhydr)oxides stable at such alkaline pH conditions. The cementation process of mine waste rocks and mine tailings gave rise to the formation mainly of C-(A)-S-H compounds, which are known to be the main hydration product of OPC, and portlandite, with its occurrence increasing with the binder:mine waste ratio. Under the alkaline conditions of these encapsulated mine wastes, both C-(A)-S-H phases and portlandite are able to fix Sb. At such pH values the external surfaces of C-(A)-S-H phases contain silanol groups which are ionized, allowing the retention of antimonate, via ternary complexes or ions pairs with calcium

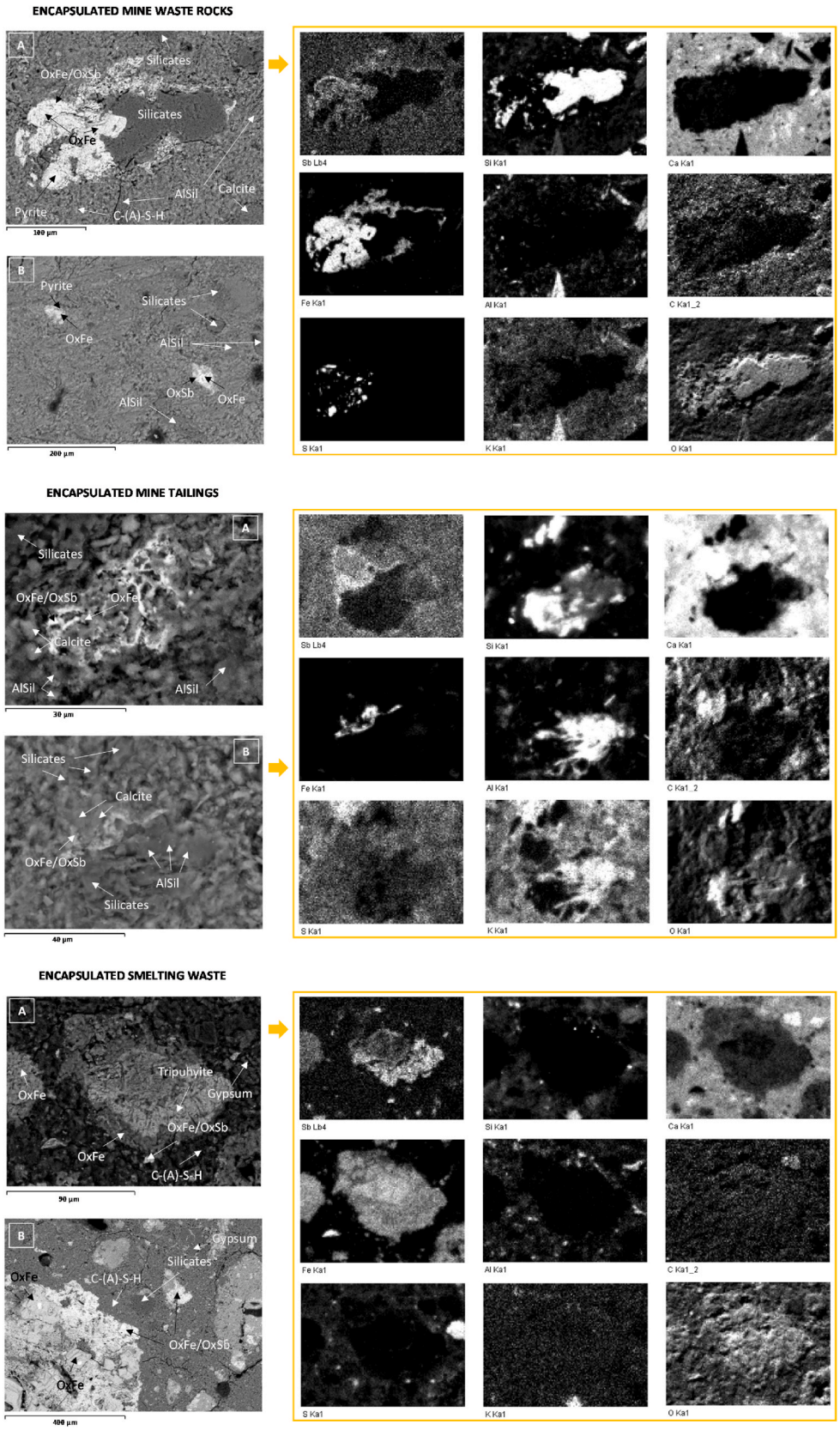

Fig. 6. SEM images and elemental distribution maps of encapsulated mine wastes using a binder:mine waste ratio of 40:60 wt% and different calcium hydroxide amounts in the binder mixture (A: 0 wt% and B: 10 wt%). (FeOx: Fe (oxyhydr)oxides, SbOx: Sb (oxyhydr)oxides, FeOx/SbOx: mixtures of Fe and Sb (oxyhydr)oxides, and AlSil: aluminosilicates).

Table 3
Spot chemical analyses of Sb-bearing phases in encapsulated mine wastes (binder:mine waste ratio of 40:60 wt% with 0 and 10 wt% of calcium hydroxide in the binder mixture).

						%				
Encapsulated waste	Phases	Sb_2O_5	SiO_2	Al_2O_3	Fe_2O_3	MgO	CaO	Na_2O	K_2O	SO_3
Mine waste rocks	Aluminosilicates (n = 5)	3.04 (2.76–3.31)	47.78 (46.64–49.13)	32.66 (29.37–35.11)	0.79 (0.36–1.89)	0.74 (0.53–1.17)	0.24 (0.06–0.53)	0.87 (0.35–1.27)	7.88 (7.43–8.65)	n.d.–0.04
	Silicates (n = 5)	0.35 (0.14–0.70)	91.47 (79.44–95.94)	5.39 (3.11–12.33)	0.13 (0.04–0.22)	0.09 (0.01–0.21)	0.09 (0.03–0.24)	0.07 (0.02–0.22)	1.25 (0.28–3.31)	n.d.–0.02
	Silicates (quartz) (n = 3)	0.03 (0.02–0.04)	98.42 (97.31–99.40)	0.58 (0.15–0.94)	0.10 (0.03–0.13)	n.d.	n.d.–0.03	n.d.–0.01	0.01 (0.01–0.02)	0.02 (0.01–0.02)
	Calcite (n = 3)	0.20 (0.18–0.21)	0.43 (0.22–0.57)	0.18 (0.15–0.24)	n.d.	n.d.	55.76 (54.60–56.81)	n.d.	0.10 (0.02–0.14)	0.01 (0.01–0.01)
	Calcite/Portlandite (n = 3)	0.14 (0.10–0.16)	0.14 (0.09–0.23)	0.90 (0.18–1.32)	1.09 (0.44–1.53)	0.21 (0.11–0.35)	59.88 (59.11–61.10)	n.d.	n.d.	n.d.
	Fe (oxyhydr)oxides (n = 4)	3.26 (0.93–5.15)	10.34 (3.96–12.60)	6.47 (0.26–9.14)	34.80 (30.43-41-92)	0.70 (0.29–0.96)	6.41 (1.16–9.55)	0.32 (0.05–0.54)	1.96 (0.12–2.88)	0.03 (0.01–0.05)
	Sb (oxyhydr)oxides (n = 6)	51.13 (34.04–58.51)	0.47 (0.20–0.90)	2.65 (0.56–7.73)	0.03 (0.02–0.06)	0.07 (0.01–0.13)	2.92 (0.12–6.58)	1.26 (0.46–1.86)	0.42 (0.14–0.52)	2.26 (0.58–4.04)
	C-(A)-S-H (n = 5)	0.13 (0.07–0.24)	25.45 (22.96–30.04)	2.53 (0.22–7.06)	6.49 (3.74–8.14)	7.36 (3.04–10.34)	24.23 (22.97–26.26)	n.d.–0.10	n.d.–0.33	0.02 (0.01–0.04)
Mine tailings	Aluminosilicates (n = 4)	1.28 (1.14–1.40)	40.10 (38.22–42.75)	31.70 (30.62–32.18)	1.40 (0.96–1.93)	0.87 (0.58–1.30)	0.76 (0.41–0.94)	0.65 (0.45–0.97)	7.14 (6.90–7.45)	0.06 (0.04–0.07)
	Silicates (quartz) (n = 5)	0.02 (0.01–0.05)	98.54 (97.54–99.52)	0.49 (0.24–0.78)	0.01 (0.01–0.02)	0.01 (0.01–0.02)	0.05 (0.02–0.08)	n.d.–0.02	n.d.–0.12	n.d.
	Calcite (n = 10)	0.20 (0.16–0.37)	0.08 (0.09–0.69)	0.16 (0.04–0.34)	0.50 (0.02–0.89)	0.48 (0.20–0.94)	55.83 (54.56–56.98)	n.d.–0.02	0.02 (0.01–0.06)	n.d.–0.16
	Calcite/Portlandite (n = 5)	0.20 (0.17–0.25)	n.d.–0.35	0.35 (0.06–0.86)	0.57 (0.13–1.29)	0.40 (0.25–0.49)	61.20 (59.69–62.67)	n.d.–0.01	0.01 (0.01–0.04)	n.d.–0.02
	Fe (oxyhydr)oxides (n = 4)	1.31 (0.71–2.96)	1.07 (0.12–1.58)	1.62 (0.38–1.88)	77.47 (72.68–81.12)	0.30 (0.10–0.44)	4.48 (1.15–6.76)	0.01 (0.01–0.01)	0.04 (0.02–0.06)	0.39 (0.17–0.53)
	Fe/Sb (oxyhydr)oxides (n = 4)	12.79 (10.80–14.25)	7.93 (4.23–9.68)	2.89 (0.95–4.14)	39.46 (33.43–45.11)	0.76 (0.50–0.96)	13.76 (9.62–17.08)	0.12 (0.06–0.20)	0.63 (0.32–0.80)	0.75 (0.54–0.98)
	C-(A)-S-H (n = 5)	0.12 (0.08–0.20)	38.26 (35.14–42.30)	8.97 (4.21–9.69)	2.21 (1.13–3.85)	4.13 (2.96–5.55)	26.02 (23.14–29.32)	0.11 (0.08–0.15)	0.18 (0.08–0.26)	0.04 (0.02–0.05)
Smelting waste	Silicates (n = 3)	0.28 (0.26–0.30)	71.59 (68.59–73.87)	1.18 (0.85–1.68)	1.37 (1.13–1.54)	0.03(0.02–0.04)	2.26 (1.46–2.90)	0.03 (0.02–0.05)	0.14 (0.07–0.20)	0.24 (0.10–0.34)
	Silicates (quartz) (n = 3)	0.02 (0.01–0.04)	97.71 (96.36–99.03)	0.44 (0.22–0.73)	0.78 (0.39–0.94)	0.13 (0.07–0.16)	0.24 (0.08–0.35)	n.d.	0.02 (0.01–0.02)	0.01 (0.01–0.01)
	Fe (oxyhydr)oxides (n = 21)	0.79 (0.09–5.26)	3.66 (0.18–15.49)	1.08 (0.27–2.95)	66.23 (50.92–95.27)	n.d.–0.21	4.68 (0.17–9.01)	n.d.–2.46	n.d.–0.69	0.07 (0.01–0.27)
	Fe(oxyhydr)oxides (hematite) (n = 4)	0.05 (0.02–0.08)	n.d.–0.20	1.97 (0.48–5.52)	96.08 (93.45–98.29)	0.54 (0.09–1.43)	0.09 (0.04–0.16)	n.d.–0.07	n.d.–0.02	n.d.
	Fe/Sb (oxyhydr)oxides (n = 4)	9.91 (8.19–11.64)	1.84 (0.18–3.50)	1.31 (0.32–2.30)	51.47 (43.86–59.07)	n.d.–0.03	4.39 (3.54–5.25)	0.56 (0.14–0.98)	0.17 (0.10–0.25)	0.08 (0.06–0.11)
	Tripuhyite (n = 4)	42.52 (34.03–51.06)	3.89 (2.33–5.48)	3.37 (0.31–6.40)	34.22 (29.63–38.89)	n.d.–0.05	2.99 (2.86–3.10)	0.91 (0.45–1.37)	0.44 (0.11–0.79)	0.07 (0.07–0.07)
	C-(A)-S-H (n = 5)	0.31 (0.23–0.44)	26.09 (23.59–31.30)	6.61 (5.67–8.48)	4.23 (3.10–5.72)	2.90 (1.77–3.92)	21.55 (14.61–27.12)	0.27 (0.16–0.34)	0.33 (0.25–0.49)	0.04 (0.03–0.05)

(Cornelis et al., 2012a). Likewise, at such pH values the adsorption of antimonate on portlandite is also favorable as its isoelectric point (12.8) is not exceeded (Cornelis et al., 2012a). At a binder:mine waste ratio of 40:60 wt% C-(A)-S-H phases and portlandite (mixed with calcite) contained on average 0.12–0.13 wt% Sb_2O_5 and 0.14–0.20 wt% Sb_2O_5, respectively, pointing out their role in attenuating the Sb release. Although detected, the presence of ettringite and hydrocalumite was too small so as to play a significant role in the retention of Sb.

As derived from the mineralogical and chemical studies, the cement encapsulation process of smelting waste provoked a progressive dissolution of natrojarosite with the increasing binder content, leading to the formation of Fe (oxyhydr)oxides. These compounds are well known scavengers of Sb; nevertheless, the adsorption of antimonate by them is favored at acidic pH and decreases importantly from circumneutral pH values as much as pH increases (Guo et al., 2014b). Therefore, the Sb attenuation capacity of newly formed Fe (oxyhydr)oxides via adsorption was restricted at the pH values of encapsulated smelting waste (approximately 8 at binder:mine waste ratios of 10:90 and 20:80 wt% and approximately 11–12 at a binder:mine waste ratio of 40:60 wt%). The cementation process of smelting waste also led to the formation of roméite and OPC hydration products, namely C-(A)-S-H phases and ettringite. The occurrence of roméite decreased with the increasing binder:mine waste ratio whereas the OPC hydration products showed the inverse trend. Roméite has shown its lower solubilities at high pH values (Cornelis et al., 2011); nevertheless, the encapsulated smelting waste where this mineral mainly occurred presented the lowest pH values, thus being unfavorable to minimize the solubilization of Sb. As the binder:mine waste ratio increased as well as did the pH values of encapsulated smelting waste, roméite gradually dissolved to form ettringite. Although ettringite has shown to remove Sb, this process has been indicated to take place by adsorption on its surface (Cornelis et al., 2012a), whereas the Sb incorporation into its structure by replacement of sulfate, that would lead to higher removal amounts of Sb, has been ruled out (Vollpracht and Brameshuber, 2016). In the encapsulated smelting waste ettringite was not identified as an Sb-carrier. By contrast, the C-(A)-S-H phases were the OPC hydration products found responsible for attenuating the release of Sb. Thus, at a binder:smelting waste ratio of 40:60 wt%, at which the leaching of Sb from encapsulated smelting waste decreased importantly, the C-(A)-S-H phases showed Sb_2O_5 contents in the range of 0.23–0.44 wt%.

4. Conclusions

The encapsulation processes based on OPC have proven their feasibility to manage the different types of mine waste (mine waste rocks, mine tailings, and smelting waste) derived from the exploitation of Sb ore deposits. A binder:mine waste ratio of 40:60 wt% was found appropriate to decrease their leachable Sb concentrations at levels below the limit for acceptance at non-hazardous waste landfills (<0.7 mg kg^{-1}) and to revert their toxic character. In the case of mine tailings, a binder:mine waste ratio of 20:80 wt% also fulfilled these aspects. The partial replacement (10–40 w%) of OPC by calcium hydroxide did not have a significant effect on the leachable Sb content at the binder:mine waste ratios found appropriate to attenuate its release, while decreased the compressive strength of derived encapsulated materials. In any case, the developed compressive strengths were higher than that regarded suitable to keep their physical integrity under the usual overburden pressures in landfills. Likewise, such materials also satisfied the compressive strength requirements for their use as fill materials. Diffusion was found the main mechanism controlling the Sb leaching from the encapsulated materials and, according to the obtained effective diffusion coefficients, these materials were suitable for disposal. Therefore, according to such leaching and strength characteristics, the encapsulated mine wastes derived under the indicated conditions could be deposited at landfills for non-hazardous waste, thus minimizing the environmental hazards caused by their accumulation in the mine surrounding areas. Alternatively, they could also be managed as mine backfill materials, although higher binder contents than those usually employed for this aim would be required if environmentally friendly backfilling is pursued. Additionally, according to the Dutch legislation on the use of waste materials in the built sector, mine tailings encapsulated using some formulations with a binder:mine waste ratio of 40:60 wt% already met the Sb leaching requirement for open construction applications. In the case of mine waste rocks and smelting waste, mixtures reducing their contents should be employed in order to decrease the leaching of Sb below the required emission standard. Therefore, Sb-bearing mine wastes, especially mine tailings, also present a great potential to be recycled as substitutes for natural aggregates in concrete in construction applications. Anyway, further research is needed in order to establish the optimum formulations as well as their long-term leachability and durability when exposed to the environment, preferentially via scaled-up experiments. After the encapsulation processes, Sb was mostly preserved in the original Sb-bearing phases [Fe (oxyhydr)oxides, Sb (oxyhydr)oxides, and tripuhyite]. The main modifications in the occurrence of Sb-bearing phases were observed in the case of smelting waste: natrojarosite was decreased, Fe (oxyhydroxides) were increased (particularly amorphous/low ordered hydrous Fe oxides), and the formation of minor amounts of roméite took place. The pH increase (from acidic to alkaline) and/or the increased calcium availability provoked by the smelting waste encapsulation process mainly accounted for such transformations. Portlandite, ettringite, hydrocalumite (really minor), and C-(A)-S-H phases were detected as hydration compounds of OPC. The latter was the predominant binding agent, playing an important role in attenuating the Sb release from the different types of mine waste; average Sb_2O_5 contents of 0.12–0.31 wt% were found in C-(A)-S-H phases.

CRediT authorship contribution statement

E. Álvarez-Ayuso: Conceptualization, Investigation, Funding acquisition, Writing - review & editing. **A. Murciego:** Investigation, Funding acquisition. **M.A. Rodríguez:** Funding acquisition. **R. Mosser-Ruck:** Funding acquisition.

Declaration of competing interest

The authors declare that they have no known competing financial interests or personal relationships that could have appeared to influence the work reported in this paper.

Data availability

Data will be made available on request.

Acknowledgments

The present study was carried out under the project TERMET (Grant number: RTI 2018-095433-B-I00) funded by Ministerio de Ciencia e Innovación (MCIN), Spain/Agencia Estatal de Investigacion (AEI), Spain and by Fondo Europeo de Desarrollo Regional (FEDER) "A way of making Europe", European Union, and the project "CLU-2019-05–IRNASA/CSIC Unit of Excellence", funded by the Junta de Castilla y León (Spain) and cofinanced by the European Union (European Regional Development Fund (ERDF) "Europe drives our growth").

References

Alloway, B.J., 1995. Heavy Metals in Soils. Blackie Academic & Professional, Glasgow.

Álvarez-Ayuso, E., 2022. Stabilization and encapsulation of arsenic-/antimony-bearing mine waste: overview and outlook of existing techniques. Crit. Rev. Environ. Sci. Technol. 52, 3720–3752.

Álvarez-Ayuso, E., Murciego, A., Rodríguez, M.A., Fernández-Pozo, L., Cabezas, J., Naranjo-Gómez, J.M., Mosser-Ruck, R., 2022. Antimony distribution and mobility in different types of waste derived from the exploitation of stibnite ore deposits. Sci. Total Environ. 816, 151566.

Álvarez-Ayuso, E., Otones, V., Murciego, A., García-Sánchez, A., Santa Regina, I., 2013. Mobility and phytoavailability of antimony in an area impacted by a former stibnite mine exploitation. Sci. Total Environ. 449, 260–268.

Anderson, C.G., 2001. Hydrometallurgically treating antimony-bearing industrial wastes. JOM 53, 18–20.

Ashley, P.M., Craw, D., Graham, B.P., Chappell, D.A., 2003. Environmental mobility of antimony around mesothermal stibnite deposits, New South Wales, Australia and Southern New Zealand. J. Geochem. Explor. 77, 1–14.

Aïtcin, P.-C., Flatt, R.J., 2016. Science and Technology of Concrete Admixtures. Elsevier Ltd, Amsterdam.

Biver, M., Shotyk, W., 2012. Stibnite (Sb_2S_3) oxidative dissolution kinetics from pH 1 to 11. Geochem. Cosmochim. Acta 79, 127–139.

Biver, M., Shotyk, W., 2013. Stibiconite (Sb_3O_6OH), senarmontite (Sb_2O_3) and valentinite (Sb_2O_3): dissolution rates at pH 2-11 and isoelectric points. Geochem. Cosmochim. Acta 109, 268–279.

Bolan, N., Kumar, M., Singh, E., Kumar, A., Singh, L., Kumar, S., Keerthanan, S., Hoang, S.A., El-Naggar, A., Vithanage, M., Sarkar, B., Wijesekara, H., Diyabalanage, S., Sooriyakumar, P., Vinu, A., Wang, H., Kirkham, M.B., Shaheen, S. M., Rinklebe, J., Siddique, K.H.M., 2022. Antimony contamination and its risk management in complex environmental settings: a review. Environ. Int. 158, 106908.

Borčinová Radková, A., Jamieson, H.E., Campbell, K.M., 2020. Antimony mobility during the early stages of stibnite weathering in tailings at the Beaver Brook Sb deposit, Newfoundland. Appl. Geochem. 115, 104528.

Bonhoure, I., Wieland, E., Scheidegger, A.M., Ochs, M., Kunz, D., 2003. EXAFS study of Sn(IV) immobilization by hardened cement paste and calcium silicate hydrates. Environ. Sci. Technol. 37, 2184–2191.

Cappuyns, V., Van Campen, A., Helser, J., 2021. Antimony leaching from soils and mine waste from the Mau Due antimony mine, North-Vietnam. J. Geochem. Explor. 220, 106663.

Carlon, C., 2007. Derivation Methods of Soil Screening Values in Europe. A Review and Evaluation of National Procedures towards Harmonisation. European Commission, Joint Research Centre, Ispra.

Chang, A.C., Pan, G., Page, A.L., Asano, T., 2002. Developing Human Health-Related Chemical Guidelines for Reclaimed Wastewater and Sewage Sludge Applications in Agriculture. World Health Organization, Geneva.

Choi, W.-H., Lee, S.-R., Park, J.-Y., 2009. Cement based solidification/stabilization of arsenic-contaminated mine tailings. Waste Manag. 29, 1766–1771.

Cornelis, G., Etschmann, B., Van Gerven, T., Vandecasteele, C., 2012a. Mechanisms and modelling of antimonate leaching in hydrated cement paste suspensions. Cement Concr. Res. 42, 1307–1316.

Cornelis, G., Gerven, T.V., Snellings, R., Verbinnen, B., Elsen, J., Vandecasteele, C., 2011. Stability of pyrochlores in alkaline matrices: solubility of calcium antimonate. Appl. Geochem. 26, 809–817.

Cornelis, G., Gerven, T.V., Vandecasteele, C., 2012b. Antimony leaching from MSWI bottom ash: modelling of the effect of pH and carbonation. Waste Manag. 32, 278–286.

Courtin-Nomade, A., Rakotoarisoa, O., Bril, H., Grybosa, M., Forestier, L., Foucher, F., Kunz, M., 2012. Weathering of Sb-rich mining and smelting residues: insight in solid speciation and soil bacteria toxicity. Chem. der Erde-Geochem. 72 (S4), 29–39.

Decree on Soil Quality, 2007. Regulation of the State Secretary for Housing, Planning and the Environment and the State Secretary for Transport. Public Works and Water Management, the Netherlands.

Elwood Madden, M.E., Madden, A.S., Rimstidt, J.D., Zahrai, S., Kendall, M.R., Miller, M. A., 2012. Jarosite dissolution rates and nanoscale mineralogy. Geochem. Cosmochim. Acta 91, 306–321.

EN-12390-3, 2020. Testing Hardened Concrete - Part 3: Compressive Strength of Test Specimens.

EN-12457-4, 2002. Characterization of Waste - Leaching-Compliance Test for Leaching of Granular Waste Materials and Sludges - Part 4: One Sstage Batch Test at a Liquid to Solid Ratio of 10 L/kg for Materials with Particle Size below 10 Mm (Without or with Size Reduction). European Committee for Standardization, Brussels.

EN-12504-1, 2020. Testing Concrete in Structures - Part 1: Cored Specimens - Taking, Examining and Testing in Compression.

European Council Decision, 2003. Council Decision 2003/33/EC of 19 December 2002 establishing criteria and procedures for the acceptance of waste at landfills pursuant to Article 16 of and Annex II to Directive 1999/31/EC. Off. J. Eur. Commun. L11, 27–49.

Feng, R., Wei, C., Tu, S., Ding, Y., Wang, R., Guo, J., 2013. The uptake and detoxification of antimony by plants: a review. Environ. Exp. Bot. 96, 28–34.

Filella, M., Belzile, N., Chen, Y.-W., 2002. Antimony in the environment: a review focused on natural waters I. Occurrence. Earth Sci. Rev. 57, 125–176.

Flaková, R., Ženišová, Z., Krčmár, D., Ondrejková, I., Sracek, O., 2017. Occurrence of antimony and arsenic at mining sites in Slovakia: implications for their mobility. Carpath. J. Earth Environ. Sci. 12, 41–48.

García-Sánchez, A., Saavedra-Alonso, J., 1983. Datos analíticos sobre cuatro patrones geoquímicos de Salamanca (Granitos S.L.) y tecnicas utilizadas. Anu. Cent. Edafol. Biol. Apl. Salamanca IX, 321–331.

Gao, W., Ni, W., Zhang, Y., Li, Y., Shi, T., Li, Z., 2020. Investigation into the semi-dynamic leaching characteristics of arsenic and antimony from solidified/stabilized tailings using metallurgical slag-based binders. J. Hazard Mater. 381, 120992.

Gu, J., Yao, J., Jordan, G., Roha, B., Min, N., Li, H., Lu, C., 2020. *Arundo donax* L. stem-derived biochar increases as and Sb toxicities from nonferrous metal mine tailings. Environ. Sci. Pollut. Res. Int. 27, 2433–2443.

Gumiel, P., Arribas, A., 1987. Antimony deposits in the iberian peninsula. Econ. Geol. 82, 1453–1463.

Guo, X., Wang, K., He, M., Liu, Z., Yang, H., Li, S., 2014a. Antimony smelting process generating solid wastes and dust: characterization and leaching behaviors. J. Environ. Sci. (China) 26, 1549–1556.

Guo, X., Wu, Z., He, M., Meng, X., Jin, X., Qiu, N., Zhang, J., 2014b. Adsorption of antimony onto iron oxyhydroxides: adsorption behavior and surface structure. J. Hazard Mater. 276, 339–345.

Harris, D.L., Lottermoser, B.G., 2006. Phosphate stabilization of polymineralic mine wastes. Mineral. Mag. 70, 1–13.

He, M., Wang, N., Long, X., Zhang, C., Ma, C., Zhong, Q., Wang, A., Wang, Y., Pervaiz, A., Shan, J., 2019. Antimony speciation in the environment: recent advances in understanding the biogeochemical processes and ecological effects. J. Environ. Sci. (China) 75, 14–39.

Islas, H., Flores, M.U., Reyes, I.A., Teja, A.M., Palacios, E.G., Pandiyan, T., Aguilar-Carrillo, J., 2020. Determination of the dissolution rate of hazardous jarosites in different conditions using the shrinking core kinetic model. J. Hazard Mater. 386, 121664.

Kabata-Pendias, A., Mukherjee, A.B., 2007. Trace Elements from Soil to Human. Springer-Verlag, Berlin.

Karimian, N., Johnston, S.G., Burton, E.D., 2017. Antimony and arsenic behavior during Fe(II)-induced transformation of jarosite. Environ. Sci. Technol. 51, 4259–4268.

Karimian, N., Johnston, S.G., Burton, E.D., 2018. Antimony and arsenic partitioning during Fe^{2+}-induced transformation of jarosite under acidic conditions. Chemosphere 195, 515–523.

Lottermoser, B.G., 2010. Mine Wastes-Characterization, Treatment and Environmental Impacts, third ed. Springer-Verlag, Berlin.

Manaka, M., Yanase, N., Sato, T., Fukushi, K., 2007. Natural attenuation of antimony in mine drainage water. Geochem. J. 41, 17–27.

Ministry of the Environment, Finland, 2007. Government Decree on the Assessment of Soil Contamination and Remediation Needs (214/2007, March 1, 2007).

Mitsunobu, S., Takahashi, Y., Terada, Y., Sakata, M., 2010. Antimony(V) incorporation into synthetic ferrihydrite, goethite, and natural iron oxyhydroxides. Environ. Sci. Technol. 44, 3712–3718.

Munksgaard, N.C., Lottermoser, B.G., 2013. Phosphate amendment of metalliferous tailings, Cannington Ag-Pb-Zn mine, Australia: implications for the capping of tailings storage facilities. Environ. Earth Sci. 68, 33–44.

Murciego, A.M., Sánchez, A.G., González, M.A.R., Gil, E.P., Gordillo, C.T., Fernández, J. C., Triguero, T.B., 2007. Antimony distribution and mobility in topsoils and plants (*Cytisus striatus, Cistus ladanifer* and *Dittrichia viscosa*) from polluted Sb-mining areas in Extremadura (Spain). Environ. Poll. 145, 15–21.

NEN 7371, 2004. Leaching Characteristics of Granular Building and Waste Materials – the Determination of the Availability of Inorganic Components for Leaching – the Maximum Availability Leaching Test. Netherlands Normalization Institute Standard.

NEN-7375, 2004. Leaching Characteristics of Moulded or Monolithic Building and Waste Materials – Determination of Leaching of Inorganic Components with the Diffusion Test – the Tank Test. Netherlands Normalization Institute Standard.

Park, I., Tabelin, C.B., Jeon, S., Li, X., Seno, K., Ito, M., Hiroyoshi, N., 2019. A review of recent strategies for acid mine drainage prevention and mine tailings recycling. Chemosphere 219, 588–606.

Roper, A.J., Williams, P.A., Filella, M., 2012. Secondary antimony minerals: phases that control the dispersion of antimony in the supergene zone. Chem. der Erde-Geochem. 72 (S4), 9–14.

Ryu, J.-G., Kim, Y., 2022. Mineral transformation and dissolution of jarosite coprecipitated with hazardous oxyanions and their mobility changes. J. Hazard Mater. 427, 128283.

Saerens, A., Ghosh, M., Verdonck, J., Godderis, L., 2019. Risk of cancer for workers exposed to antimony compounds: a systematic review. Int. J. Environ. Res. Publ. Health 16, 4474.

Salihoglu, G., 2014. Immobilization of antimony waste slag by applying geopolymerization and stabilization/solidification technologies. J. Air Waste Manag. Assoc. 64, 1288–1298.

Schwarz-Schampera, U., 2014. Antimony. In: Gunn, G. (Ed.), Critical Metals Handbook. John Wiley & Sons, Ltd., Hoboken, N.J., pp. 70–98

Tommaseo, C.E., Kersten, M., 2002. Aqueous solubility diagrams for cementitious waste stabilization systems. 3. Mechanism of zinc immobilizaton by calcium silicate hydrate. Environ. Sci. Technol. 36, 2919–2925.

Tóth, G., Hermann, T., Da Silva, M.R., Montanarella, L., 2016. Heavy metals in agricultural soils of the European Union with implications for food safety. Environ. Int. 88, 299–309.

Verbeeck, M., Moens, C., Gustafsson, J.P., 2021. Mechanisms of antimony ageing in soils: an XAS study. Appl. Geochem. 128, 104936.

Vink, B.W., 1996. Stability relations of antimony and arsenic compounds in the light of revised and extended Eh-pH diagrams. Chem. Geol. 130, 21–30.

Vollpracht, A., Brameshuber, W., 2016. Binding and leaching of trace elements in Portland cement pastes. Cement Concr. Res. 79, 76–92.

Wilson, S.C., Lockwood, P.V., Ashley, P.M., Tighe, M., 2010. The chemistry and behaviour of antimony in the soil environment with comparisons to arsenic: a critical review. Environ. Poll. 158, 1169–1181.
Yilmaz, E., Belem, T., Benzaazoua, M., 2014. Effects of curing and stress conditions on hydromechanical, geotechnical and geochemical properties of cemented paste backfill. Eng. Geol. 168, 23–37.
Zahrai, S.K., Elwood Madden, M.E., Madden, A.S., Rimstidt, J.D., 2013. Na-jarosite dissolution rates: the effect of mineral composition on jarosite lifetimes. Icarus 223, 438–443.
Zhang, Y., Lu, X., Yu, R., Li, J., Miao, J., Wang, F., 2022. Long-term leachability of Sb in smelting residue stabilized by reactive magnesia under accelerated exposure to strong acid rain. J. Environ. Manag. 301, 113840.